Aerosol Speciation Using UV-Vis Observations by DSCOVR/EPIC

Alexei Lyapustin, NASA GSFC
Sujung Go (UMBC), Myungje Choi (UMBC),
G. Schuster (NASA LARC)

CEOS Atmospheric Composition Virtual Constellation AC-VC-17

June 7-11, 2021

Earth Polychromatic Imaging Camera (EPIC)

- 2048 x 2048 pixel CCD;
- 8 km pixel; 2x2 onboard aggr.
- Number of daytime images
  - 6 in winter (same area)
  - Up to 12 in summer

Wavelength (nm)	Full width (nm)	Primary Applications
317.5 ±0.1	*1 ±0.2*	*Ozone, SO_2*
325 ±0.1	*2 ±0.2*	*Ozone*
340 ±0.3	*3 ±0.6*	*Ozone, Aerosols*
388 ±0.3	*3 ±0.6*	*Aerosols, Clouds*
443 ±1	*3 ±0.6*	*Aerosols*
551 ±1	*3 ±0.6*	*Aerosols, Vegetation*
680 ±0.2	*2 ±0.4*	*Aerosol, Vegetation, Clouds*
687.75 ±0.2	*0.8 ±0.2*	*Cloud Height*
764.0 ±0.2	*1 ±0.2*	*Cloud Height*
779.5 ±0.3	*2 ±0.4*	*Clouds, Vegetation*

Aerosol Retrieval
Atmospheric Correction

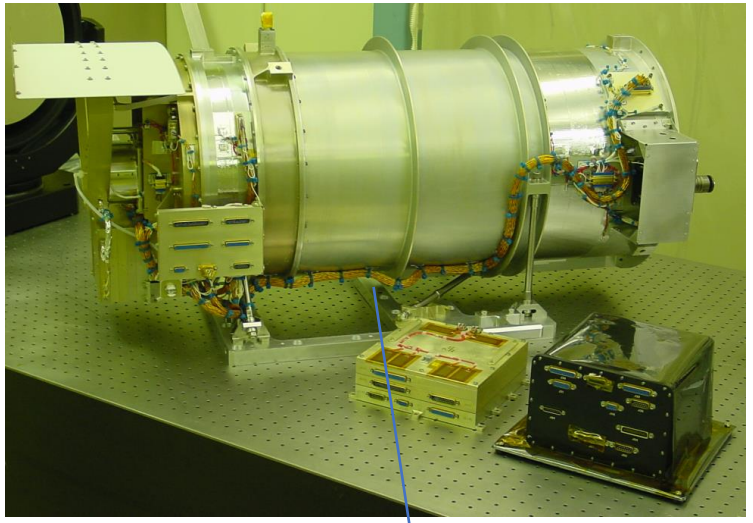

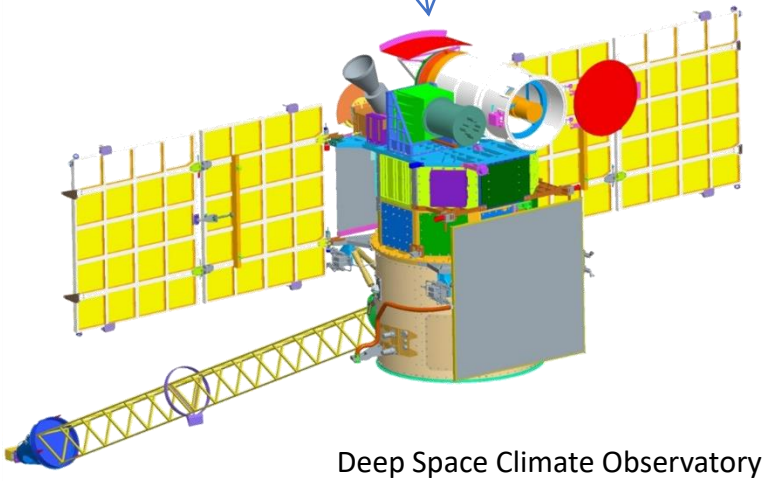

Deep Space Climate Observatory (DSCOVR)

On orbit since 2015

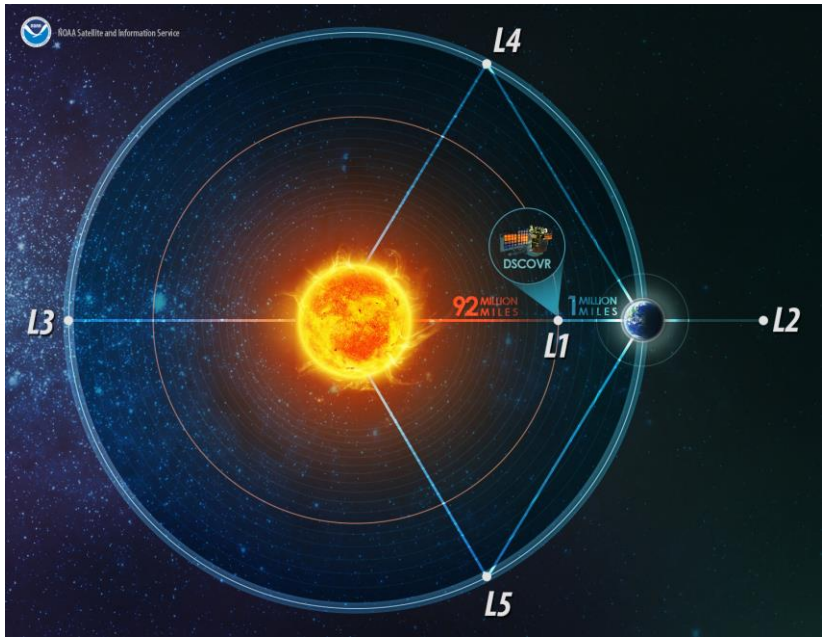

MAIAC EPIC v2 Joint Retrieval Algorithm

- Minimum Reflectance Method to characterize spectral SR ratio at 340, 388, 443 and 680nm in 4 SZA bins

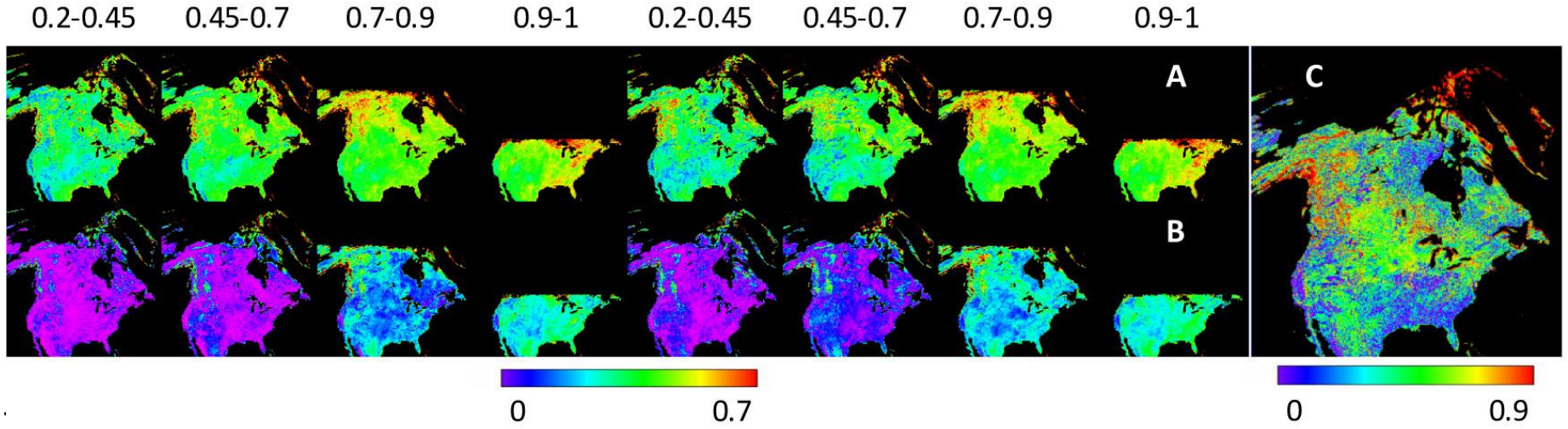

Example for NA:
(A) 443/680nm
(B) 388/680nm
(C) 340/388nm

- Absorption model (imaginary ref. index): $k_\lambda = k_0 (\lambda/\lambda_0)^{-b}$ for $\lambda < \lambda_0$, where λ_0 = 680nm
  (*in the limit of small particles, AAE~b+1, where Absorption Ångström Exponent AAE is defined for the AAOD*).
- Real *refIM* and size distribution are fixed. The results are reported for H^a=1 and 4km for smoke and dust.
- Retrieve {AOD, k_0, b} using Levenberg-Marquart optimal fit of 340, 388, 443 and 680nm:

$$F^2 = 1/N \sum \left(\frac{L^m_\lambda - L^t_\lambda}{L^m_\lambda}\right)^2 = \min\{AOD_{443}, k_0, b\}$$

- LUT-based retrievals on a 4x4 matrix of b={0.1, 1.5, 3, 4} and k_0 ={0.001, 0.006, 0.011, 0.016} - smoke
  {0.0006, 0.0014, 0.0022, 0.003} - dust.

Summary SSA_{443} Validation: 2018

Smoke, North America

H^a=1km H^a=4km

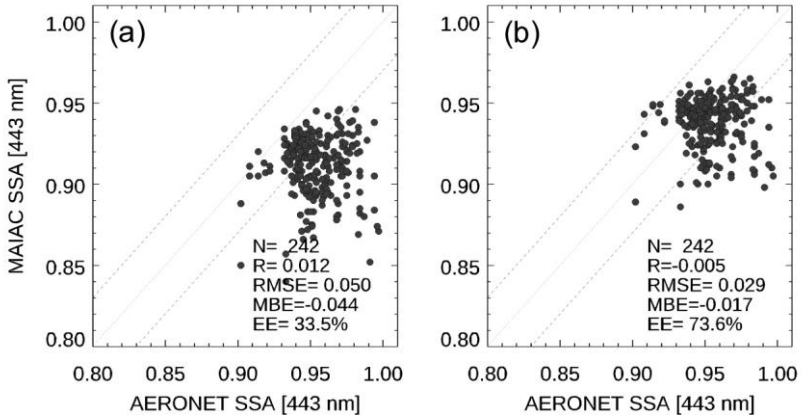

Dust: North Africa/Arabia/Middle East

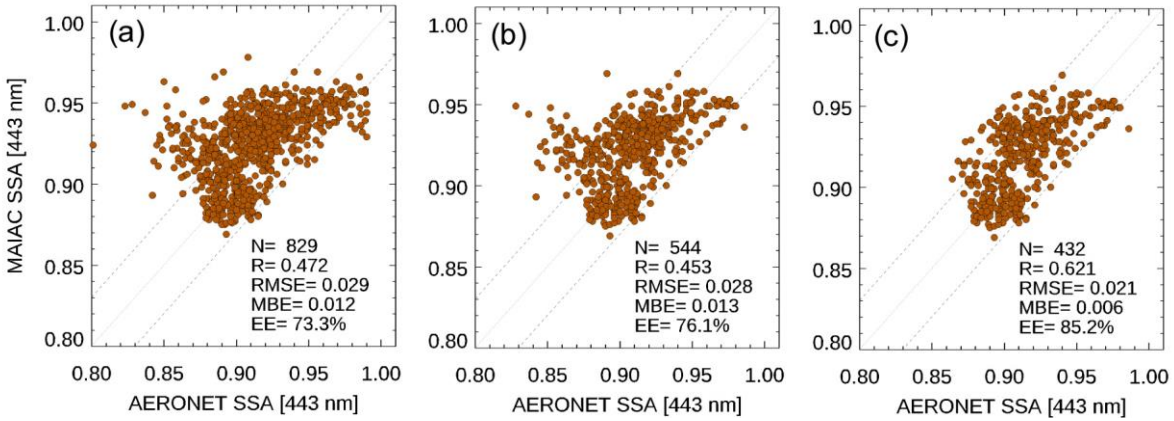

(A,B) 17 sites, AERONET AOD_{440} > 0.4 and > 0.6.

(C) 15 sites (AOD_{440} > 0.6), with Cairo_ENM_2 and Ilorin excluded.

Spectral Dependence of Absorption

Following Figure 3 and Figure 4 of Schuster et al (2016)

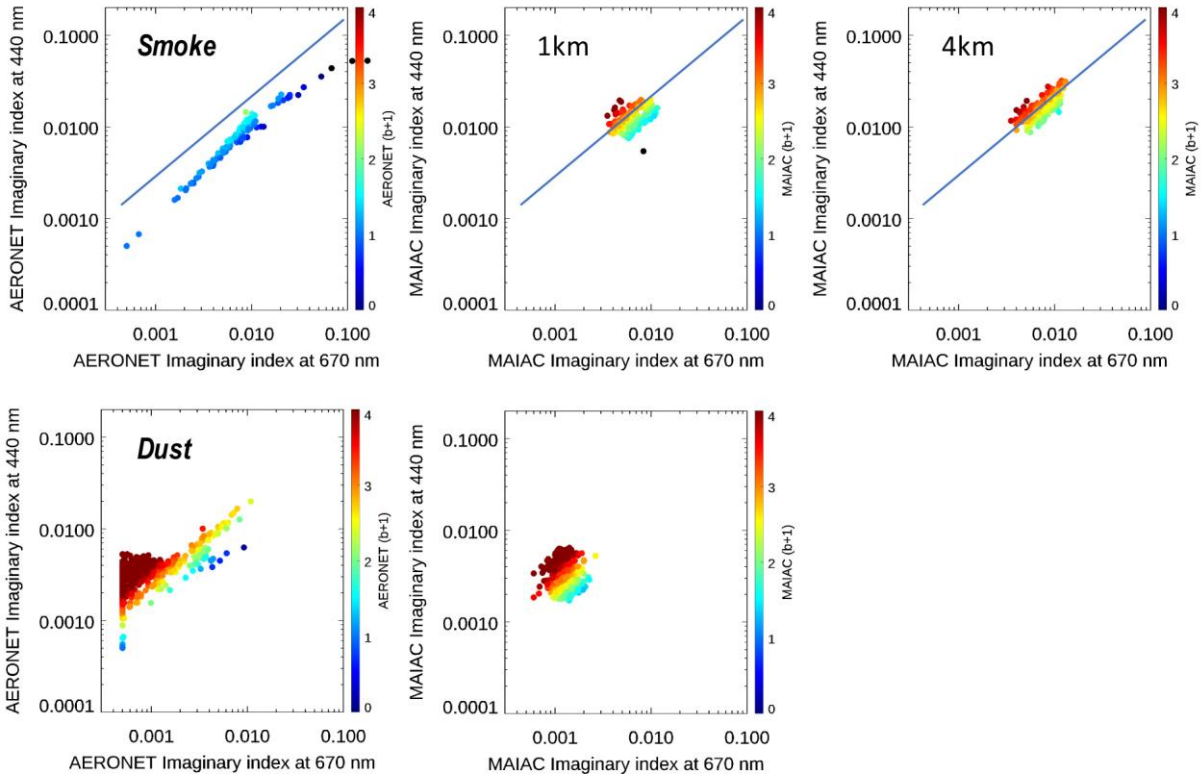

Smoke: MAIAC EPIC *b* is higher than AERONET

(this is expected from UV compared to AERONET's Blue-1020nm)

Dust: EPIC and AERONET *b* are similar

Lyapustin A., Go S., Korkin S., Wang Y., Torres O., Jethva H. and Marshak A. (2021) Retrievals of Aerosol Optical Depth and Spectral Absorption From DSCOVR EPIC. *Front. Remote Sens*. 2:645794. doi: 10.3389/frsen.2021.645794.

Inferring iron oxide species in mineral dust aerosols

(follow Schuster et al., 2016)

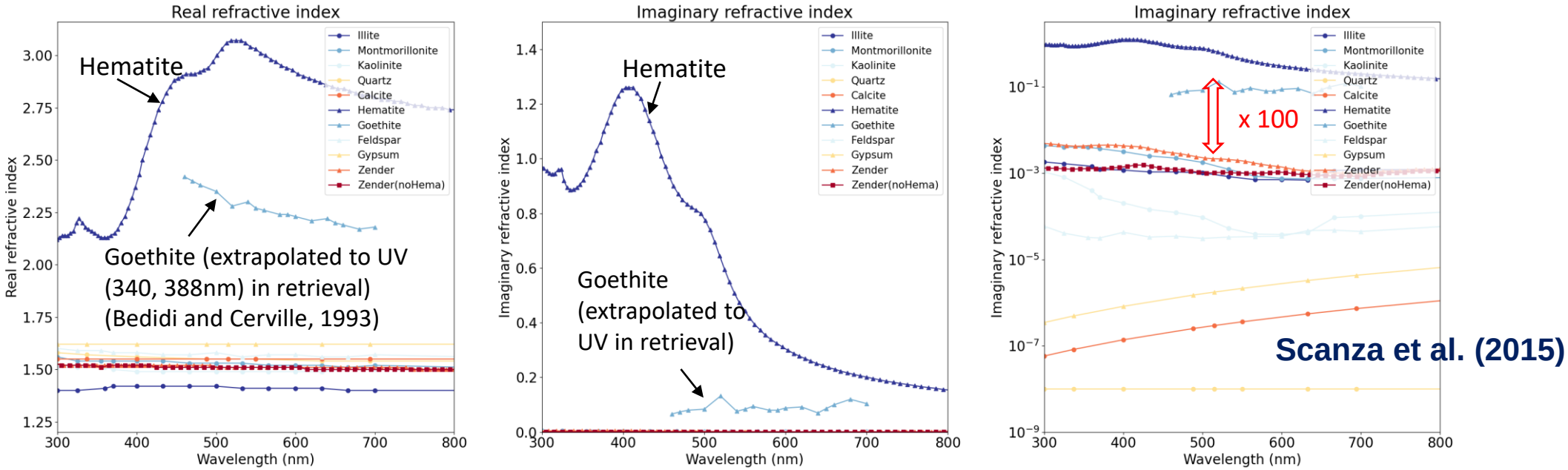

Scanza et al. (2015)

- Hematite (α-Fe_2O_3) and goethite (α-FeOOH), both in the Fe(Ⅲ) oxidation state, are the major iron oxides species in mineral dust (Torrent et al., 1983). They are major components controlling the absorption signal magnitude of pure dust toward SW radiation [e.g., Sokolik and Toon,1999; Moosmüller et al., 2012; Lafon et al., 2006; Formenti et al., 2014], as can be inferred from their complex refractive index imaginary part characteristics (Fig.1).

- We inferred hematite (α-Fe_2O_3) / goethite (α-FeOOH) content for major global dust source regions from MAIAC EPIC L2 products.

Methodology - (Forward)

(1) With known refractive index ($\boldsymbol{n}, \boldsymbol{k}$) or complex dielectric function ($\boldsymbol{\varepsilon_r}$, $\boldsymbol{\varepsilon_i}$)

$$\varepsilon_1 = \varepsilon_{1,r} + i\varepsilon_{1,i} = (n_1^2 - k_1^2) + i(2n_1k_1)$$
$$\varepsilon_2 = \varepsilon_{2,r} + i\varepsilon_{2,i} = (n_2^2 - k_2^2) + i(2n_2k_2)$$
$$\varepsilon_h = \varepsilon_{h,r} + i\varepsilon_{h,i} = (n_h^2 - k_h^2) + i(2n_hk_h)$$

, where 1, 2, h indicates inclusion 1 (hematite), inclusion 2 (goethite), and host

(2) Maxwell Garnett effective medium approximation (f_1, f_2 : volume fraction of inclusions)

$$\varepsilon_{MG} = \varepsilon_h \left[1 + \frac{3\left(f_1\frac{\varepsilon_1-\varepsilon_h}{\varepsilon_1+2\varepsilon_h} + f_2\frac{\varepsilon_2-\varepsilon_h}{\varepsilon_2+2\varepsilon_h}\right)}{1 - f_1\frac{\varepsilon_1-\varepsilon_h}{\varepsilon_1+2\varepsilon_h} - f_2\frac{\varepsilon_2-\varepsilon_h}{\varepsilon_2+2\varepsilon_h}}\right] = \varepsilon_{MG,r} + i\varepsilon_{MG,i}$$

$$n_{mix} = \sqrt{\frac{\sqrt{{\varepsilon_{MG,r}}^2 + {\varepsilon_{MG,i}}^2} + \varepsilon_{MG,r}}{2}} \quad , k_{mix} = \sqrt{\frac{\sqrt{{\varepsilon_{MG,r}}^2 + {\varepsilon_{MG,i}}^2} - \varepsilon_{MG,r}}{2}}$$

$$\Rightarrow \quad m_{mix}(\lambda_j) = F(f_1, f_2, m_1(\lambda_j), m_2(\lambda_j), n_{host}(\lambda_j))$$
$$= n_{mix}(\lambda_j) + ik_{mix}(\lambda_j)$$

Illustration of Maxwell Garnett effective medium approximation (**pure dust**)
(Bohren and Huffman, 1987; Schuster et al., 2016)

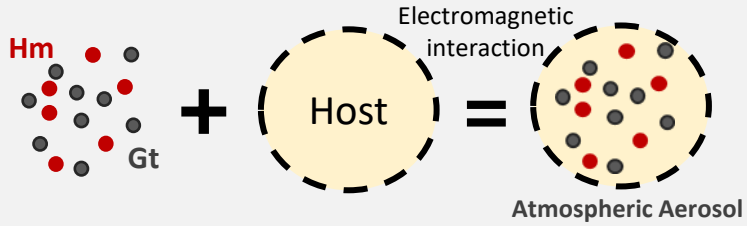

- **Assumption:** major absorption caused by hematite and goethite (not host)
- n_h = 1.52 (fixed), k_h = 0.0
- λ_j : 340, 388, 443, 680 nm
- **Fitting k_{epic} part only,** because MAIAC EPIC does not retrieve real refractive index (n_{epic})

- (Inversion)

$$\chi^2 = \sum_{j=1}^{4}\left[\frac{(k_{epic}(\lambda_j) - k_{mix}(\lambda_j))^2}{k_{epic}(\lambda_j)}\right] \rightarrow min$$

MAIAC EPIC refractive index ($k_{epic}(\lambda_j) = k_{680}\,(\lambda_j/\lambda_{680})^{-b}$)
Updated iteratively

From EPIC AOD to composition mass concentration

- Step 1: calculate total (fine + coarse) volume concentration of dust (440 nm)
  - $\tau^a = \tau_f^a + \tau_c^a = C_{Vf}h_f + C_{Vc}h_c \approx C_{Vc}h_c$ ($\because C_{Vf} \ll C_{Vc}$ for AOD>0.6)
  - With $h_c = 1.2526$, $C_V \approx C_{Vc} = \frac{\tau^a}{1.2526} = 0.7983 * \tau^a$
  - C_V: volume concentration (μm^3/μm^2)
  - h_c: AOD per unit volume concentration

Volume concentration (μm^3/μm^2):

$$C_{\mathrm{V}} = \int_{r_{\min}}^{r_{\max}} \frac{dV(r)}{d\ \ln r}\, d\ \ln r.$$

- Step 2: separate Hematite/Goethite volume concentration (C_V) using retrieved volume fraction (f) results
  - $C_{V,hematite} = C_V * f_{hematite}$
  - $C_{V,goethite} = C_V * f_{goethite}$
  - $C_{V,host} = C_V * f_{host} = C_V * (1 - f_{hematite} - f_{goethite})$

- Step 3: Then, calculate Hematite/Goethite mass concentration (C_M)
  - $C_{M,Hematite} = C_{V,Hematite} * \rho_{Hematite}$ ($\rho_{Hematite}$= mass concentration per unit volume (or density) = 5260 kg/m^3)
  - $C_{M,Goethite} = C_{V,Goethite} * \rho_{Goethite}$ ($\rho_{Goethite}$= 3800 kg/m^3)
  - $C_{M,Host} = C_{V,Host} * \rho_{Host}$ ($\rho_{Host} = \rho_{Zender}$ *= 2500 kg/m^3)

    * Zender (Mahowald et. al., 2006) assuming Maxwell–Garnett mixing of 47.6 % quartz, 25 % illite, 25 % montmorillonite, 2 % calcite and 0.4 % hematite by volume with density equal to 2500 kg/m^3 and hygroscopicity prescribed at 0.14 (Scanza et al., 2015).

    * Density of free iron is roughly twice that of other minerals (Schuster et al., 2016; Formenti et al., 2014).

  - ex) τ^a=0.75, $f_{hematite}$= 0.005

$$C_{M,Hematite} = \frac{\tau^a}{1.2526} * f_{hematite} * \rho_{Hematite} = \frac{0.75}{1.2526} * 0.005 * 5260 = 15.74\ [\mathrm{mg/m^2}]$$

Dust episodes - Sahara / Sahel

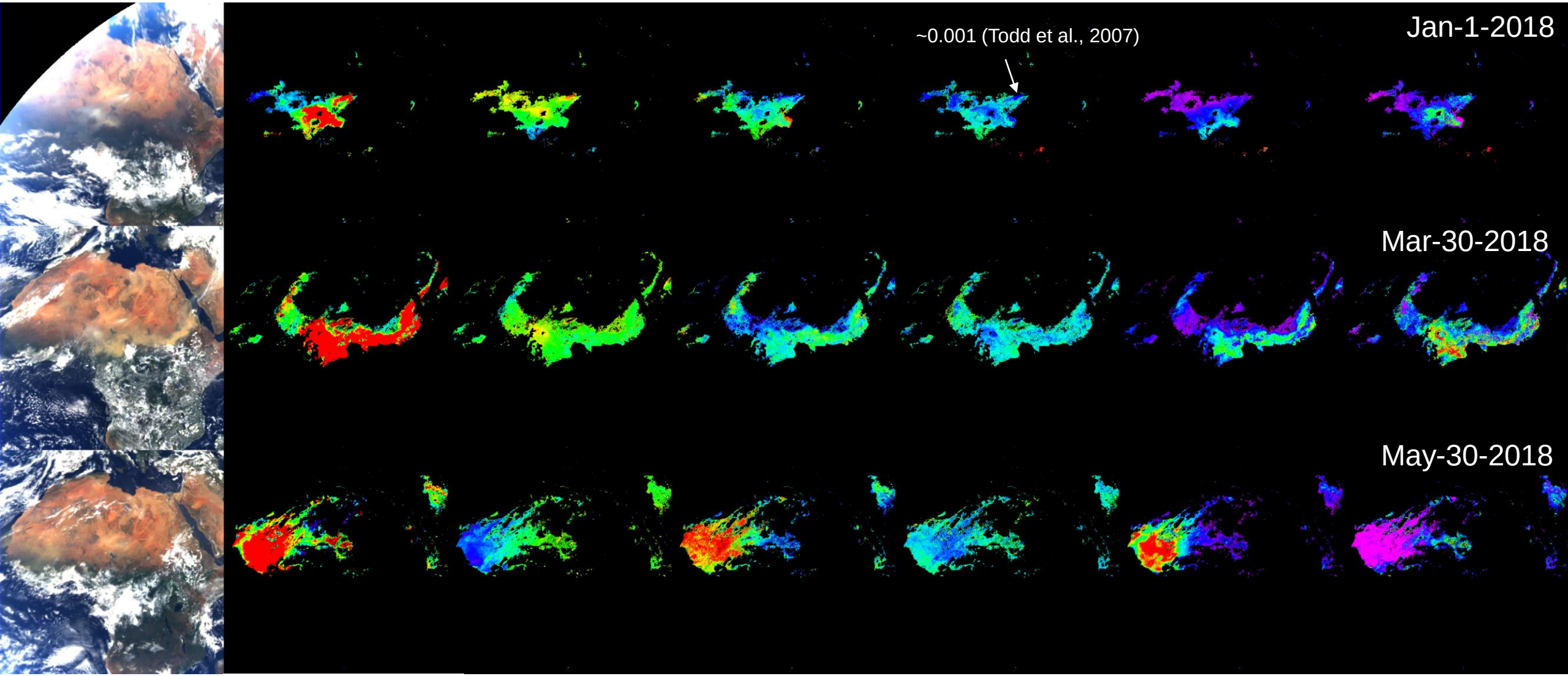

Comparison with Di Biagio et al. (2019)

- **Shaded area : EPIC retrieved**
  - Hematite / Goethite
  - 5th, median, 95th
  - With pixels of AOD>1.0 used only
  - ± 1 degree box pixels collected (Monthly)
  - 01/01/2018 – 12/31/2018 (1 year)
  - **Soil content + affected by transport due to different source regions**

- **Dashed line : Di Biagio et al. (2019)**
  - ± 10% uncertainty
  - Simulation chamber study (with X-ray absorption near edge structure (XANES) method), from soil samples and sediments collected from each desert area
  - Refer to the bulk composition of pure dust aerosol in dry condition with a size range of 2-6day transport.
  - **Soil content only**

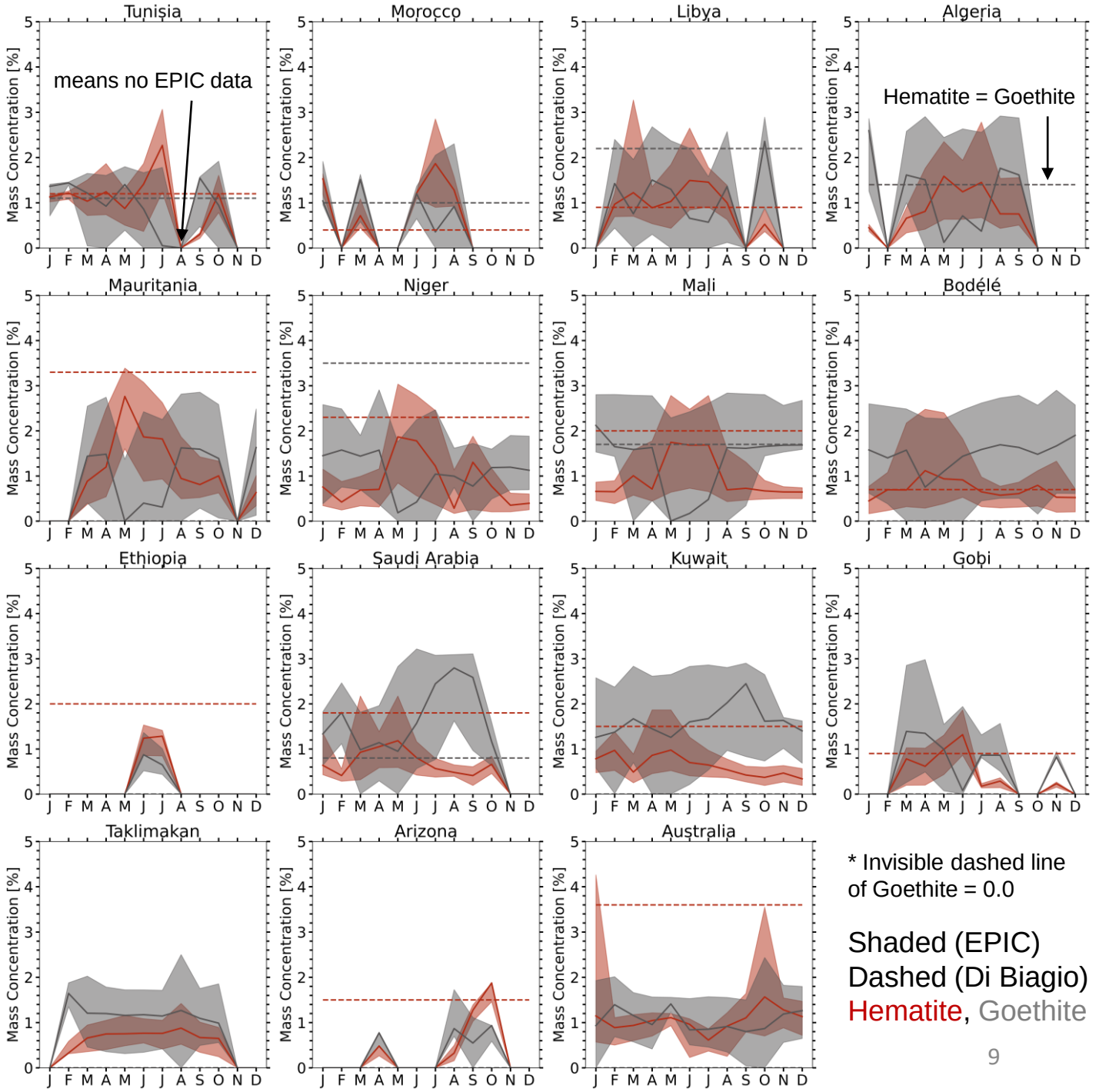

* Invisible dashed line of Goethite = 0.0

Shaded (EPIC)
Dashed (Di Biagio)
Hematite, Goethite

Climatology of iron oxides species

- Pixels of AOD>1.0 used only
- 01/01/2018 – 12/31/2018 (1 year)

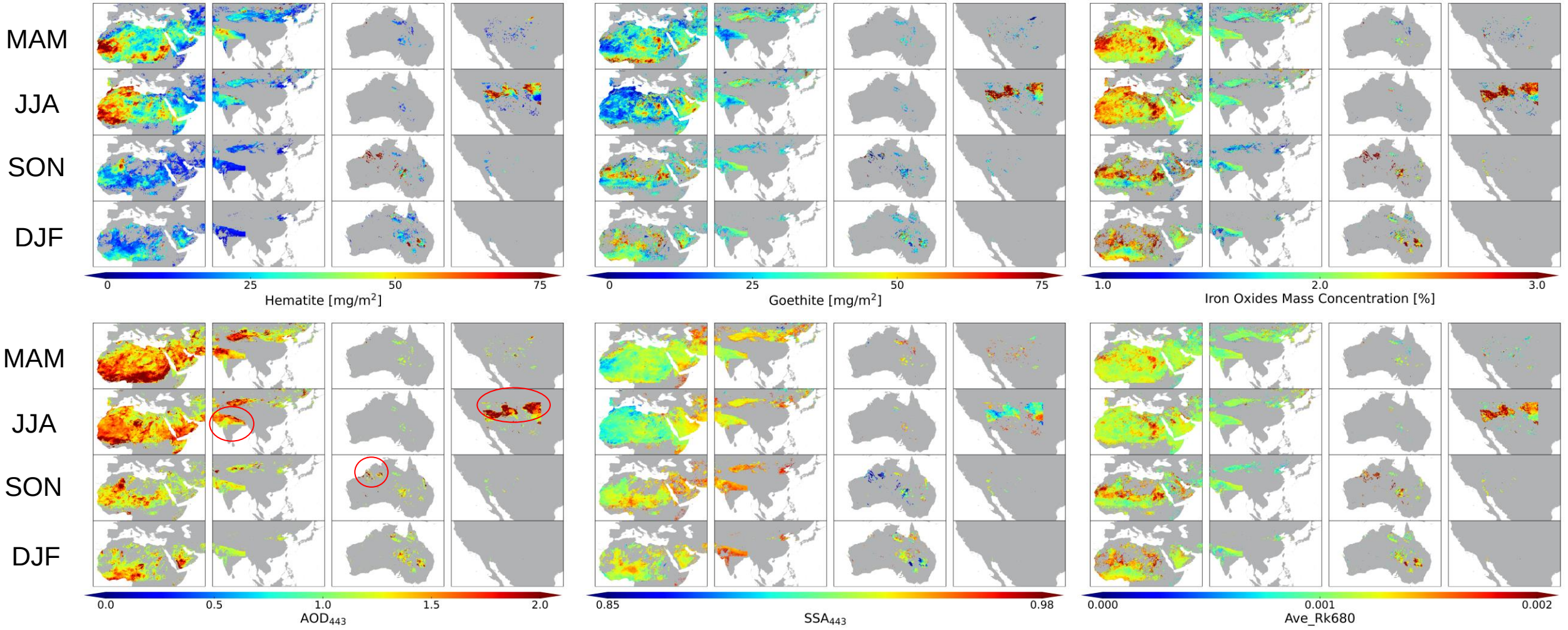

(April)

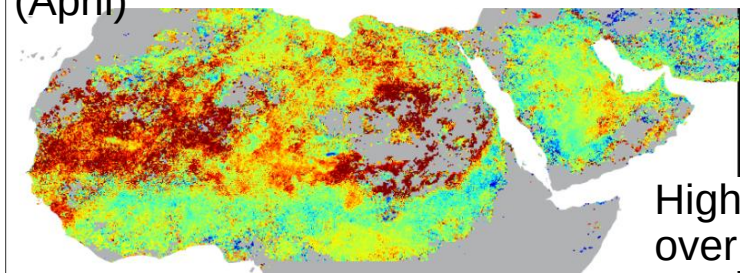

High Iron oxide over Sahel

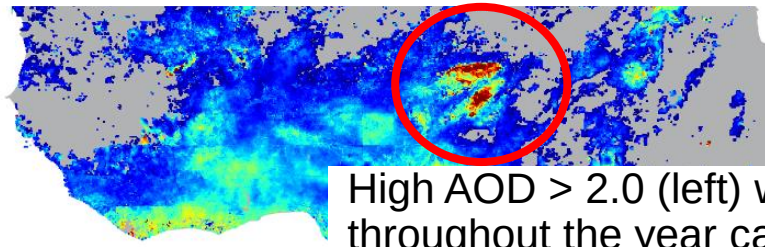

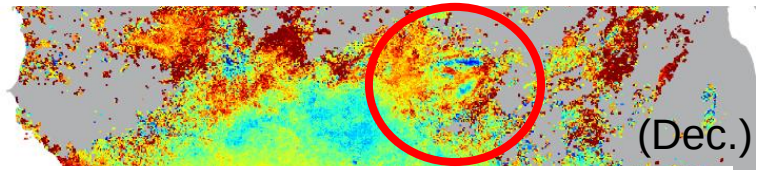

(Dec.)

High AOD > 2.0 (left) with low iron oxides content ~1% (right) throughout the year captured over Bodélé.

Conclusions

- **MAIAC EPIC DSCOVR v2 features:**
  - New joint retrieval of AOD and spectral absorption
  - Good SSA accuracy, R~0.62, rmse~0.02, bias ~0.006 (dust) and rmse~0.029, EE=73.6% (smoke @ 4km) (AERONET SSA uncertainty ±0.03)
  - Resolve spatial variations of absorption, in particular for Spectral Absorption Exponent (SAE, b)

Lyapustin A., Go S., Korkin S., Wang Y., Torres O., Jethva H. and Marshak A. (2021) Retrievals of Aerosol Optical Depth and Spectral Absorption From DSCOVR EPIC. *Front. Remote Sens*. 2:645794. doi: 10.3389/frsen.2021.645794.

- **Global Analysis of Hematite/Goethite in Mineral Dust Based on (AOD, k_0, b):**
  - Retrieved iron oxides enveloped the overall range of Di Biagio et al. (2019) soil measurement data of iron oxides 0.7-5.8% and were in line with the previous published results
  - Hematite/Goethite ratio shows significant seasonal and spatial variability
  - Initial Climatology of Hematite and Goethite content is provided

Go, S., A. Lyapustin, G. Schuster et al. Inferring iron oxides content in mineral dust aerosols from DSCOVR EPIC (to be submitted).

- **Similar Analysis of Black/Brown Carbon for Biomass Burning Aerosol is Coming Soon**